Cell. Mol. Life Sci. (2014) 71:1775–1788
DOI 10.1007/s00018-013-1471-5

Cellular and Molecular Life Sciences

RESEARCH ARTICLE

Role of the ubiquitin–proteasome system in the regulation of $P2Y_{13}$ receptor expression: impact on hepatic HDL uptake

Véronique Pons · Nizar Serhan · Stéphanie Gayral · Camille Malaval · Michel Nauze · Nicole Malet · Muriel Laffargue · Céline Galés · Laurent O. Martinez

Received: 9 July 2013 / Revised: 28 August 2013 / Accepted: 30 August 2013 / Published online: 13 September 2013

Abstract The protective effect of high density lipoproteins (HDL) against atherosclerosis is mainly attributed to their capacity to transport excess cholesterol from peripheral tissues back to the liver for further elimination into the bile, a process called reverse cholesterol transport (RCT). Recently, the importance of the $P2Y_{13}$ receptor ($P2Y_{13}$-R) was highlighted in HDL metabolism since HDL uptake by the liver was decreased in $P2Y_{13}$-R deficient mice, which translated into impaired RCT. Here, we investigated for the first time the molecular mechanisms regulating cell surface expression of $P2Y_{13}$-R. When transiently expressed, $P2Y_{13}$-R was mainly detected in the endoplasmic reticulum (ER) and strongly subjected to proteasome degradation while its homologous $P2Y_{12}$ receptor ($P2Y_{12}$-R) was efficiently targeted to the plasma membrane. We observed an inverse correlation between cell surface expression and ubiquitination level of $P2Y_{13}$-R in the ER, suggesting a close link between ubiquitination of $P2Y_{13}$-R and its efficient targeting to the plasma membrane. The C-terminus tail exchange between $P2Y_{13}$-R and $P2Y_{12}$-R strongly restored plasma membrane expression of $P2Y_{13}$-R, suggesting the involvement of the intra-cytoplasmic tail of $P2Y_{13}$-R in expression defect. Accordingly, proteasomal inhibition increased plasma membrane expression of functionally active $P2Y_{13}$-R in hepatocytes, and consequently stimulated $P2Y_{13}$-R-mediated HDL endocytosis. Importantly, proteasomal inhibition strongly potentiated HDL hepatic uptake (>200 %) in wild-type but not in $P2Y_{13}$-R-deficient mice, thus reinforcing the role of $P2Y_{13}$-R expression in regulating HDL metabolism. Therefore, specific inhibition of the ubiquitin–proteasome system might be a novel powerful HDL therapy to enhance $P2Y_{13}$-R expression and consequently promote the overall RCT.

Keywords G-protein coupled receptor · Ubiquitination · BRET assay · Reverse cholesterol transport · Lipoproteins

Introduction

Several prospective studies have established that the plasma level of high density lipoprotein (HDL) cholesterol (HDL-C) is an independent negative risk factor for coronary heart diseases and thus represents a major protective factor against atherosclerosis. HDL exert direct vasculoprotective functions through their anti-inflammatory, anti-oxidant, anti-thrombotic and cyto-protective properties, but their main atheroprotective action is attributed to their metabolic role in reverse cholesterol transport (RCT), a process whereby excess cell cholesterol is taken up from peripheral cells (cholesterol efflux), processed into HDL particles, and then later delivered to the liver (cholesterol

Electronic supplementary material The online version of this article (doi:10.1007/s00018-013-1471-5) contains supplementary material, which is available to authorized users.

V. Pons · N. Serhan · S. Gayral · C. Malaval · M. Nauze · N. Malet · M. Laffargue · C. Galés · L. O. Martinez
INSERM, UMR 1048, Institut des Maladies Métaboliques et Cardiovasculaires, Toulouse 31432, France

L. O. Martinez
e-mail: Laurent.Martinez@inserm.fr

V. Pons · N. Serhan · S. Gayral · C. Malaval · M. Nauze · N. Malet · M. Laffargue · C. Galés · L. O. Martinez
Université de Toulouse III, UMR 1048, Toulouse 31300, France

V. Pons (✉) · L. O. Martinez
INSERM U1048, Bât. L3, Hôpital Rangueil, BP 84225, 31432 Toulouse cedex 03, France
e-mail: veronique.pons@inserm.fr

uptake) for further metabolism and bile excretion. Reverse cholesterol transport relies on specific interactions between HDL particles and both peripheral cells and hepatocytes. Among cellular proteins interacting with HDL, some contribute to the cholesterol efflux such as cellular ATP binding cassette transporters ABCA1 and ABCG1 [1], whereas others are involved in hepatic HDL cholesterol uptake. To date, two distinct cell surface receptors are known to contribute to HDL uptake by the liver: (1) the scavenger receptor class B type I (SR-BI) that is involved in selective uptake of cholesterol ester from HDL [2], and (2) the membrane-associated ecto-F_1-ATPase identified as a high affinity receptor for the major protein component of HDL, apolipoprotein A-I (apoA-I), and involved in the uptake of both protein and lipid moieties of the HDL particles, a process called HDL holoparticle endocytosis [3]. Basically, apoA-I binds the ecto-F_1-ATPase at the cell surface of hepatocytes, promoting ATP hydrolysis into ADP which in turn leads to subsequent activation of a G-protein coupled receptor (GPCR)—namely $P2Y_{13}$ receptor ($P2Y_{13}$-R). $P2Y_{13}$-R activation leads to a Rho/ROCKI signaling pathway and actin cytoskeleton reorganization that eventually stimulate HDL holoparticle endocytosis through an unknown low affinity receptor that is different from SR-BI [3–5].

We and others recently highlighted the physiological importance of $P2Y_{13}$-R in vivo since RCT was impaired in mice deficient for $P2Y_{13}$-R [6, 7]. Conversely, in vivo $P2Y_{13}$-R activation by bolus injection of its partial agonist Cangrelor (AR-C69931MX) increased biliary lipid secretions in wild-type but not $P2Y_{13}$-R knock-out mice [6]. Similarly, chronic pharmacological activation of $P2Y_{13}$-R by Cangrelor in mice increased hepatic HDL uptake and bile acid secretion [8]. Thus, $P2Y_{13}$-R appears as a promising pharmacological target in the field of emergent HDL therapies aiming at modulating RCT and treating/preventing the development of atherosclerosis. Interestingly, nowadays, an important concept is that increasing HDL-C levels may not necessarily be the optimal target for the development of new therapies targeted toward HDL, because the protective ability of HDL may be more related to cholesterol elimination through the RCT pathway. Thus, some new therapeutic approaches are now focusing on promoting RCT, without necessarily raising HDL-C levels per se, supporting the notion that the function of HDL is more important than its concentration. Therefore, therapies that improve HDL "function", even if they do not increase HDL-C levels, may have important anti-atherogenic and vascular protective effects. With this in mind, we hypothesized that enhancing $P2Y_{13}$-R expression at the cell surface of hepatocytes could be highly relevant to increasing HDL hepatic uptake and consequently promoting RCT and cholesterol elimination.

$P2Y_{13}$-R belongs to the GPCR family and shares a high homology sequence with $P2Y_{12}$ receptor ($P2Y_{12}$-R), another ADP receptor, as well as similar functional features such as Gαi protein coupling [9]. In addition to cholesterol metabolism, $P2Y_{13}$-R has also been implicated in other physiological processes, including neuronal differentiation [10], insulin secretion [11], mast cell degranulation [12], ATP release by red blood cells [13], or bone homeostasis [14]. However, so far, the molecular mechanisms that regulate trafficking and cell surface expression of $P2Y_{13}$-R have not been investigated.

In this study, we investigated for the first time the regulation of cell surface expression of $P2Y_{13}$-R. To our surprise, we found that $P2Y_{13}$-R exhibited poor general protein expression as well as poor cell surface expression in different cell types when compared to $P2Y_{12}$-R. Interestingly, we demonstrated that $P2Y_{13}$-R was subjected to a constitutive ubiquitination in the endoplasmic reticulum (ER), thus promoting proteasome-mediated receptor degradation, and thereby preventing its expression at the plasma membrane. Finally, we also demonstrated that proteasomal inhibition, which drastically increased cell surface expression of $P2Y_{13}$-R in HepG2 cells, greatly potentiated $P2Y_{13}$-R-mediated hepatic HDL endocytosis in vivo, thus giving promising applications for future improvements for HDL therapies.

Materials and methods

Constructs and reagents

$P2Y_{13}$ (NCBI Reference Sequence: NM_176894), $P2Y_{12}$ (NCBI Reference Sequence: NM_022788) and chimerical receptors were amplified by PCR and subcloned into pEGFP-N1, pRLuc8-N1 or fused myc epitope. $P2Y_{12}$ cDNA was a generous gift from C. Gachet (UMR-S949 INSERM, Strasbourg, France) and Ub-GFP[2] construct was a generous gift from M. Bouvier (University of Montréal, Montréal, Canada). MG-132 was purchased from Sigma (St. Louis, MO, USA) and bortezomib from Sequoia Research Products (Berkshire, UK).

Cell culture and transfection

HeLa cells (human cervix adenocarcinoma), HepG2 cells (human liver hepatocellular carninoma) and HEK293T cells (human embryonic kidney) were maintained in DMEM Glutamax (Sigma) supplemented with 10 % fetal bovine serum (Life Technologies) and 100 µg/mL penicillin/streptomycin in a humidified atmosphere containing 5 % CO_2. HepG2 cells were grown on collagen I-coated dishes. Transient transfections were performed using X-tremeGENE 9

DNA Transfection Reagent (Roche Applied Science) for HeLa and HepG2 cells and using polyethylenimine (PEI, Polysciences) for HEK293T cells.

Quantification of cell surface receptors by ELISA

Cells were split into 24-well plates and transiently transfected with pcDNA3.1 (+) (control) or vectors encoding N-terminally myc-tagged receptors. Twenty-four hours post-transfection, cells were treated or not with proteasome inhibitors as indicated for 16 h at 37 °C. The,n cells were fixed in 4 % paraformaldehyde, saturated with PBS containing 1 % bovine serum albumin and incubated with the primary anti-myc antibody (Clone 9E10; Santa Cruz Biotechnology) and then with HRP-labeled secondary antibody (Sigma). After washing, cells were incubated with HRP substrate: TMB (3,39,5,59-tetramethylbenzidine). The reaction was stopped with HCl 1 N, and the plates were read at 450 nm in a microplate reader (Varioscan Flash, Thermo Electron). The 570- nm optic density (background) was subtracted.

Microscopy

Cells were fixed in 4 % paraformaldehyde, permeabilized with 0.05 % saponin when necessary, saturated with PBS containing 10 % fetal bovine serum and incubated with the primary antibody and then with Cy3-labeled secondary antibody (Jackson Immunoresearch Laboratories). Pictures were captured using a Zeiss LSM 710 META confocal microscope equipped with a ×63 Plan-Apochromat objective.

Western blot

For protein analysis, cell lysates (50 μg) were subjected to SDS-PAGE electrophoresis under reducing conditions, transferred onto PVDF membranes (Millipore), and analyzed by immunoblotting according to standard protocols using indicated antibodies. We used a mouse monoclonal antibody against Myc (clone 9E10) from BD Biosciences, and a mouse monoclonal antibody against GAPDH from Santa Cruz Biotechnology. HRP-labeled secondary antibodies were from Sigma.

Cell fractionation

Cell fractionation was performed as previously described [15]. Briefly, cells were washed with cold PBS, scraped off, and lysed with cold hypotonic lysis buffer (20 mM HEPES, pH 7.4; 2 mM EDTA; 2 mM EGTA; 6 mM magnesium chloride) containing protease inhibitors. After homogenization using a tight-fitting dounce, and removal of cellular debris and unlysed cells by centrifugation, the supernatant was adjusted to a final concentration of 0.2 M sucrose. A discontinuous sucrose step gradient was made using lysis buffer. Cell lysate was applied to the top of discontinuous sucrose step gradient (0.5, 0.9, 1.2, 1.35, 1.5, and 2 M) and centrifuged for 16 h at 130,000*g*. Fractions were then subjected to fluorescence/luminescence analysis and to BRET measurements.

Bioluminescence resonance energy transfer measurement

Constructs encoding RLuc8-fused receptors and GFP^2-tagged ubiquitin were transiently cotransfected into HEK293T cells as indicated in the figure legends. Forty-eight hours after transfection, cells were washed with PBS and resuspended in PBS containing 0.1 % (w/v) glucose at room temperature. Cells were then distributed (80 μg of proteins per well) in a 96-well microplate (Wallac, PerkinElmer Life and Analytical Sciences). $BRET^2$ between RLuc8 and GFP^2 was measured after the addition of the RLuc8 substrate coelenterazine 400a (5 μM, Interchim). $BRET^2$ readings were collected using a modified Infinite F500 (Tecan). The BRET signal was calculated by the ratio of emission of GFP^2 (510–540 nm) to RLuc8 ($BRET^2$, 370–450 nm).

Fluorescent HDL endocytosis

HDL were fluorescently labeled with Alexa Fluor® 568 dye according the instructions of manufacturer (Life technologies). Then, 100 μg/mL Alexa Fluor® 568-HDL particles were endocytosed for 15 min at 37 °C in HepG2 cells. Cells were washed 3 times in serum-free DMEM, and then dissociation of extracellular membrane-bound HDL was performed at 4 °C in serum-free DMEM for 90 min. Following washes, cells were fixed using 4 % paraformaldehyde and examined using an Olympus IX81 microscope. Quantification was done using Image J software.

Perfused mouse liver experiments

C57BL/6 wild-type mice and $P2Y_{13}$-$R^{-/-}$ littermates were used in this study, as previously described [6]. Mice were caged in animal rooms with alternating 12 h periods of light (0700–1900 hours) and dark (1900–0700 hours) and fed ad libitum with a normal mouse chow diet (# R04-10; SAFE, France). All animal procedures were performed in accordance with the guidelines of the Committee on Animals of the Midi-Pyrénées Ethics Committee on Animal Experimentation and with the French Ministry of Agriculture license. For experiments, mice (10–12 weeks old) were treated twice at a 5-day interval with 0.5 mg/kg of bortezomib or the vehicle (PBS) by subcutaneous injection. Five

days after the second injection, mice were anesthetized by intraperitoneal injection of ketamine hydrochloride and xylazine hydrochloride. The liver was perfused in situ for 10 min at 37 °C with PBS (Invitrogen) containing 50 µg proteins/mL of ^{125}I-HDL3 (specific radioactivities ranged from 1,000 to 1,500 cpm/ng of proteins). Livers were extensively washed at 4 °C in PBS and radioactivity associated with the liver was counted ($n \geq 6$ per group).

Results

$P2Y_{13}$ receptor is poorly expressed and does not exhibit cell surface expression

To investigate cell surface expression of $P2Y_{13}$-R, we first tagged the receptor with a myc epitope in N-terminus extracellular region (Myc-$P2Y_{13}$) and transiently expressed the construct in HeLa cells. Surprisingly, Myc-$P2Y_{13}$ was detected at very low levels and in only a few cells (Fig. 1a). Interestingly, when detected, Myc-$P2Y_{13}$ receptor was rarely found at the plasma membrane and mostly localized in the endoplasmic reticulum (ER) as shown by the colocalization with DsRed2-ER marker (Fig. 1b). By contrast, when overexpressed, Myc-$P2Y_{12}$ receptor, another ADP receptor, was strongly detected in almost all the cells and exhibited efficient plasma membrane targeting (Fig. 1a).

We further confirmed these observations by precisely quantifying total expression of each receptor as well as receptor density at the plasma membrane. For that purpose, we fused $P2Y_{13}$ or $P2Y_{12}$ receptors either with a Renilla luciferase tag (RLuc8) in their C-terminus region or with a myc epitope in N-terminus extracellular region as mentioned above. After transfection of identical amounts of the different receptor-encoding vectors, luciferase luminescence was measured as an indicator of total receptor expression (Fig. 1c) while cell surface density of myc-tagged receptors was classically determined by ELISA and revealed with an anti-myc antibody on non-permeabilized cells (Fig. 1d). In agreement with fluorescence imaging experiments, the results showed a huge difference in receptor expression levels between $P2Y_{13}$ and $P2Y_{12}$ receptors. Indeed, $P2Y_{13}$-R was poorly expressed (Fig. 1c), and almost not detected at the plasma membrane (Fig. 1d) compared to $P2Y_{12}$-R. To rule out any variations in transfection efficiency between vectors encoding $P2Y_{13}$ and $P2Y_{12}$ receptors which could in part support receptor expression differences, we quantified cell surface expression of both $P2Y_{12}$ and $P2Y_{13}$ receptors following transfection of increasing amounts of each encoding vector (Fig. 1e). While detection of $P2Y_{12}$-R was increased with increasing amounts of encoding vector until reaching a plateau, $P2Y_{13}$-R was still undetectable, even after transfection with the highest amount of encoding vector (Fig. 1e). Similar results were obtained when the two P2Y receptors were expressed in other cell lines, including HepG2 cells, indicating that the regulation of $P2Y_{13}$-R expression did not depend on the cell type (Supplementary Fig. S1).

Altogether, these data demonstrate that $P2Y_{13}$-R is poorly expressed, and mostly retained in the ER.

$P2Y_{13}$ receptor expression is regulated through its C-terminal tail

$P2Y_{13}$-R displays high homology sequence with $P2Y_{12}$-R, especially in transmembrane domains, and alignment between $P2Y_{13}$-R and $P2Y_{12}$-R amino acid sequences reveals that both receptors share ~50 % identity and ~70 % homology. The highest variability is found in the C-terminus cytoplasmic tail, which is known to regulate GPCR trafficking and expression (Fig. 2a). To evaluate the influence of the C-terminus tail of $P2Y_{13}$-R in cell surface expression of this receptor, we constructed two chimeric receptors consisting of the exchange of the C-terminus tail of $P2Y_{13}$ and $P2Y_{12}$ between the two receptors, namely $P2Y_{13\text{-}12}$ ($P2Y_{13}$-R core domain containing the C-terminus tail of $P2Y_{12}$-R) and $P2Y_{12\text{-}13}$ ($P2Y_{12}$-R core domain containing the C-terminus tail of $P2Y_{13}$-R) (Fig. 2b). Wild-type and chimeric receptors were C-terminally fused to GFP or RLuc8 and next transiently expressed in HeLa cells to investigate expression levels of the receptors. Strikingly, the replacement of the C-terminus tail of $P2Y_{13}$-R by the one of $P2Y_{12}$-R strongly increased general expression of $P2Y_{13}$-R (Fig. 2c, d) and restored its cell surface expression (Fig. 2c), suggesting that the cytoplasmic tail of $P2Y_{13}$-R was involved in the specific expression defect of this receptor. Conversely, the $P2Y_{12\text{-}13}$ chimera total expression was significantly reduced compared to $P2Y_{12}$-R expression (Fig. 2d), thus demonstrating that the C-terminus tail of $P2Y_{13}$-R could drive the degradation of a part of $P2Y_{12}$-R. Cell surface expression of myc-tagged receptors was further quantified by ELISA experiments (Fig. 2e) and revealed by using an anti-myc antibody on non-permeabilized cells. Again, and in agreement with fluorescence imaging, $P2Y_{13}$-R expression at the plasma membrane was markedly and significantly increased when its C-terminus tail was replaced by the one of $P2Y_{12}$-R. However, whereas the replacement of the C-terminus tail of $P2Y_{12}$-R by the one of $P2Y_{13}$-R decreased total expression level of $P2Y_{12}$-R, it did not impact on $P2Y_{12}$-R cell surface expression (Fig. 2d, e), suggesting that the C-terminal of $P2Y_{13}$-R was most probably regulating receptor expression in the ER rather than receptor cell surface trafficking per se.

Altogether, these data demonstrated that the expression of $P2Y_{13}$-R is tightly regulated through its C-terminus intra-cytoplasmic tail.

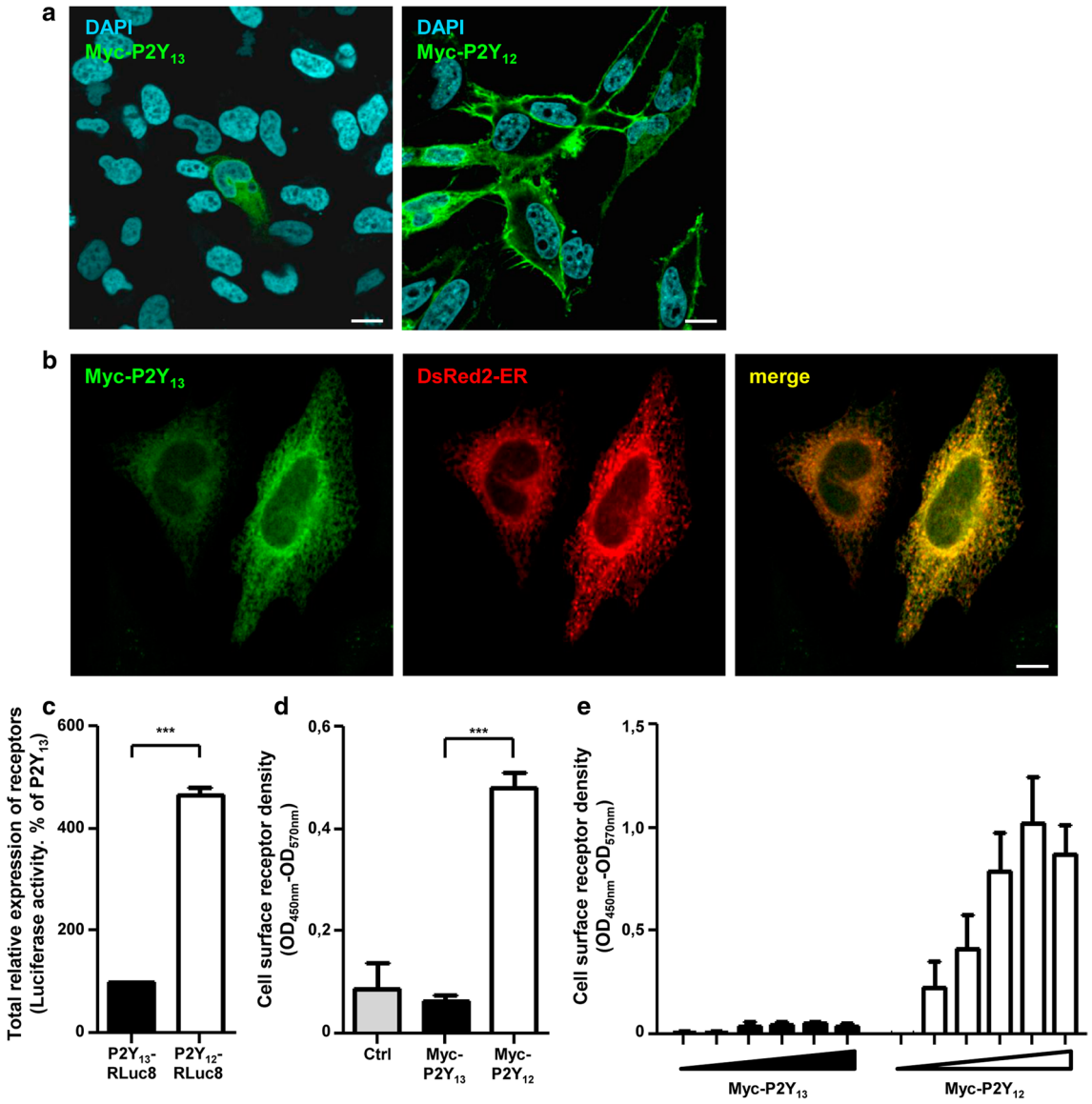

Fig. 1 $P2Y_{13}$ receptor is poorly expressed and does not exhibit cell surface expression. **a** HeLa cells expressing N-terminally Myc-tagged $P2Y_{13}$ or $P2Y_{12}$ were processed for immunofluorescence using an anti-myc antibody. Nuclei were stained with 5 μg/mL DAPI. *Scale bar* 10 μm. **b** HeLa cells co-expressing Myc-$P2Y_{13}$ and the ER marker, DsRed2-ER, were processed for immunofluorescence using an anti-myc antibody. Nuclei were stained with 5 μg/mL DAPI. *Scale bar* 10 μm. **c** HEK293T cells were transfected with identical amounts of DNA constructs encoding RLuc8-tagged receptors and luciferase intensity was measured 48 h after transfection. Results are expressed as the mean ± SEM of at least three independent experiments and analyzed by paired *t* test (***$p < 0.001$). **d** HeLa cells expressing Myc-tagged $P2Y_{13}$ or $P2Y_{12}$ were analyzed by ELISA using an anti-myc antibody to quantify cell surface expression of the different receptors. Results are expressed as the mean of at least three independent experiments and analyzed by paired *t* test (***$p < 0.001$). Standard errors are indicated. **e** HeLa cells were transfected with increasing amounts of vectors encoding N-terminally Myc-tagged $P2Y_{13}$ or $P2Y_{12}$ (ranging from 15 to 500 ng/well). Then, cell surface expression of the different receptors was analyzed by ELISA using an anti-myc antibody. Results are expressed as the mean of at least three independent experiments. Standard errors are indicated

$P2Y_{13}$ receptor is constitutively ubiquitinated at steady state

The ER constitutes the limiting compartment for GPCR maturation and thus expression. Generally, misfolded transmembrane receptors in the ER then become ubiquitinated to finally undergo proteasomal degradation [16]. Given the propensity of $P2Y_{13}$-R to naturally limit its expression in the ER, we thus hypothesized that expression of $P2Y_{13}$-R might be regulated through ubiquitination of its C-terminus tail. To test this hypothesis, we monitored the real-time ubiquitination of the $P2Y_{13}$-R and $P2Y_{12}$-R in

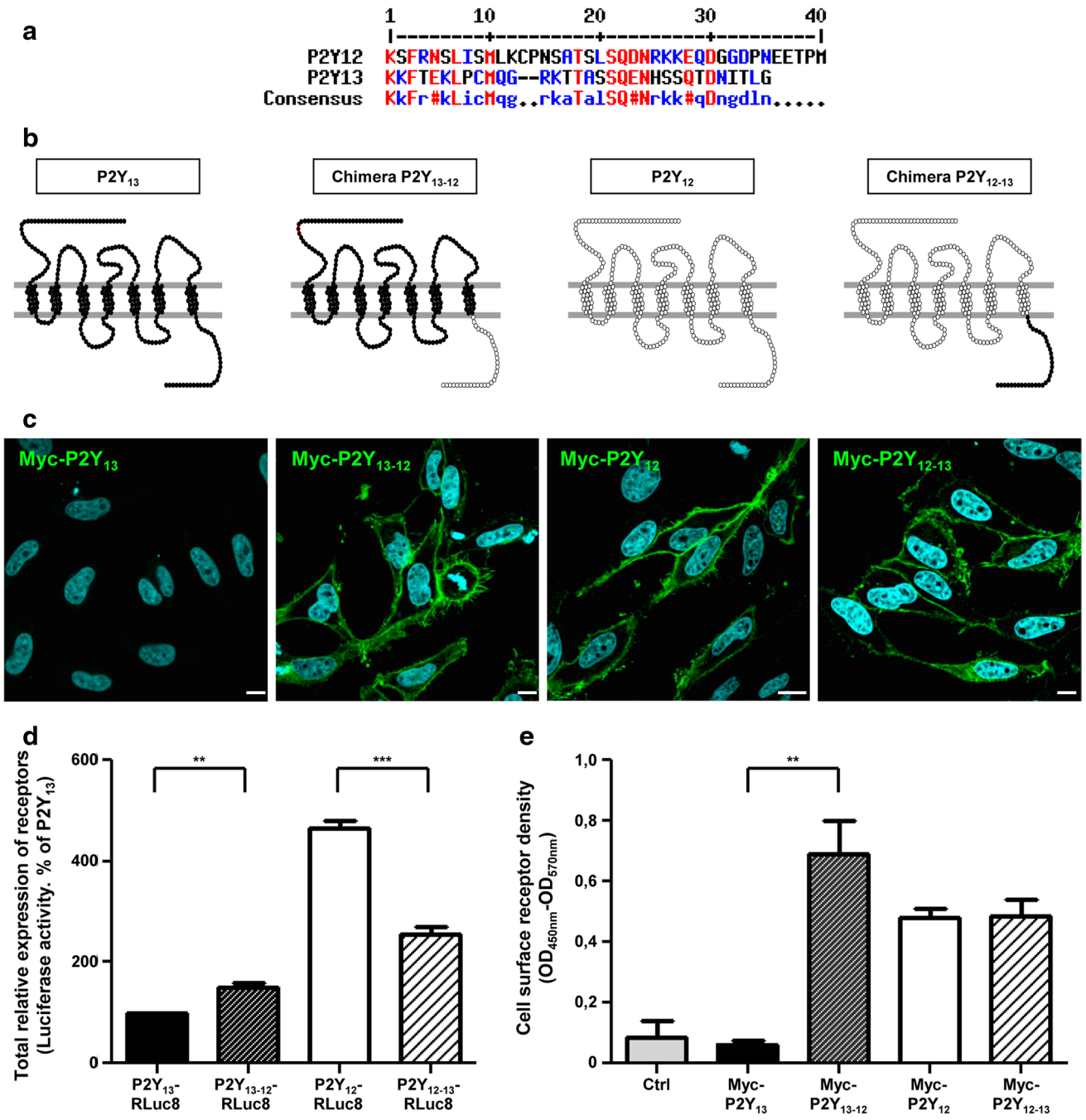

Fig. 2 Surface expression of $P2Y_{13}$ receptor is regulated through its C-terminal tail. **a** Alignment of amino acid sequences of the C-terminus tail of human $P2Y_{12}$ and $P2Y_{13}$. **b** Schematic representation of $P2Y_{13}$, $P2Y_{12}$ as well as chimerical receptors consisting of the exchange of the C-terminus tail of $P2Y_{13}$ and $P2Y_{12}$ receptors. **c** HeLa cells expressing N-terminally Myc-tagged $P2Y_{13}$, $P2Y_{12}$ or the two chimeras $P2Y_{13\text{-}12}$ or $P2Y_{12\text{-}13}$ were processed for immunofluorescence using an anti-myc antibody. Nuclei were stained with 5 μg/mL DAPI. *Scale bar* 10 μm. **d** HEK293T cells were transfected with identical amounts of DNA constructs encoding RLuc8-tagged $P2Y_{13}$, $P2Y_{12}$ or the two chimeras $P2Y_{13\text{-}12}$ or $P2Y_{12\text{-}13}$ and luciferase intensity was measured 48 h after transfection. Results are expressed as the mean ± SEM of at least three independent experiments and analyzed by paired *t* test (**$p < 0.005$, ***$p < 0.001$). **e** HeLa cells expressing N-terminally Myc-tagged $P2Y_{13}$, $P2Y_{12}$ or the two chimeras $P2Y_{13\text{-}12}$ or $P2Y_{12\text{-}13}$ were analyzed by ELISA using an anti-myc antibody to quantify cell surface expression of the different receptors. Results are expressed as the mean of at least three independent experiments and analyzed by paired *t* test (**$p < 0.005$). Standard errors are indicated

living cells using $BRET^2$ (Bioluminescence Resonance Energy Transfer)-based ubiquitination probes as previously described [17]. This assay is based on the nonradiative transfer of energy between a luminescent energy donor (here, Renilla luciferase, RLuc8) fused to the protein of interest and a fluorescent energy acceptor (here, green fluorescent protein, GFP^2) fused to the N-terminus of ubiquitin (GFP^2-Ub), which has been previously successfully used to study the dynamic ubiquitination of signaling proteins [17]. Therefore, to monitor $P2Y_{13}$-R and $P2Y_{12}$-R ubiquitination, wild-type and chimeric $P2Y_{13}$ and $P2Y_{12}$ receptors were fused to their C-terminal to RLuc8 and receptor ubiquitination was measured using the GFP^2-Ub fusion protein (Fig. 3a). We first performed saturation BRET curves [18] in HEK293T cells by co-expressing a constant level of $P2Y_{13}$-RLuc8 or $P2Y_{12}$-RLuc8 encoding vector with increasing concentrations of GFP^2-Ub. As shown in Fig. 3b, a basal $BRET^2$ signal could be detected between $P2Y_{13}$-R and ubiquitin which increased hyperbolically as a function of the GFP^2-Ub expression level and saturated at high GFP^2-Ub concentration, thus demonstrating the specificity of the BRET signal, and consequently that $P2Y_{13}$-R undergoes constitutive ubiquitination (Fig. 3b). By contrast, a very weak $BRET^2$ signal was detected when experiments were performed with $P2Y_{13}$-RLuc8 receptor and soluble GFP^2 as a negative control. This BRET signal is independent of the GFP^2 expression level leading to linear saturation BRET curves, most likely reflecting bystander BRET (random collision) (Fig. 3b). Similar results were obtained when measuring ubiquitination of $P2Y_{12}$-R, indicating that $P2Y_{12}$-R also undergoes basal ubiquitination (Fig. 3c). However, it is noteworthy that the basal BRET ratio between $P2Y_{12}$-R-RLuc8 and GFP^2-Ub was much lower than that measured in the presence of $P2Y_{13}$-R, which could be indicative of less $P2Y_{12}$-R basal ubiquitination.

Interestingly, when BRET was measured between $P2Y_{13\text{-}12}$ chimeric receptor and GFP^2-Ub, the signal was significantly decreased when compared to wild-type $P2Y_{13}$-R. Conversely, when considering $P2Y_{12\text{-}13}$ receptor, the ubiquitination was significantly increased compared to wild-type $P2Y_{12}$ (Fig. 3d). The differences in the BRET signals detected between GFP_2-Ub and the different P2Y receptors could not rely on variations in receptor expression since all $BRET^2$ experiments were performed using similar luminescence levels indicative of receptor expression (Fig. 3d, see inset).

Altogether, these results indicated that $P2Y_{13}$-R, and most likely its C-terminus tail, was highly ubiquitinated at steady state when compared to $P2Y_{12}$-R. Moreover, the data showed an inverse correlation between cell surface expression and ubiquitination level of $P2Y_{13}$-R, suggesting a close link between ubiquitination of $P2Y_{13}$-R and its efficient targeting to the plasma membrane.

$P2Y_{13}$ receptor is ubiquitinated in the endoplasmic reticulum

BRET signals measuring ubiquitination of P2Y receptors were conducted on intact cells and thus cannot provide direct information on the subcellular localization of the detected interactions. Therefore, we performed BRET measurements after cell fractionation using sucrose step gradient to determine the precise location of the $P2Y_{13}$-R ubiquitination. After cell membrane solubilization and fractionation, luciferase intensity (Fig. 4a) and $BRET^2$ assay (Fig. 4b) were assessed on each fraction to detect $P2Y_{13}$-R expression and ubiquitination, respectively. The gamma-aminobutyric acid (GABA) B receptor R1 (GABA B-R1), another GPCR which is retained in the ER [19], was used as an index of ER membrane enrichment while $P2Y_{12}$-R represents an indicator of the plasma membrane (PM)-enriched fractions. As expected, $P2Y_{12}$-R was mainly found in fractions 4–6 whereas GABA B-R1 was mainly detected in fractions 7–10, thus delineating the distribution of PM- and ER-enriched fractions, respectively (Fig. 4a). Despite low expression, $P2Y_{13}$-R could be detected in both PM- and ER-enriched fractions (Fig. 4a). Interestingly, when we measured BRET between $P2Y_{13}$-RLuc8 and GFP^2-Ub on sucrose fractions, we observed that $BRET^2$ signal was mostly detected in ER-enriched fractions—and not in PM-enriched fractions—(Fig. 4b), demonstrating that ubiquitination of $P2Y_{13}$-R occurred mainly in the ER.

Proteasome inhibition induces expression of $P2Y_{13}$ receptor at the cell surface of human hepatocytes

Since proteasomal proteolysis is closely linked to the ubiquitination of the target molecules for degradation, we analyzed whether $P2Y_{13}$-R was degraded through proteasome by using specific inhibitors. After proteasomal inhibition with MG-132, a strong expression of $P2Y_{13}$-GFP was observed in almost all the cells (Fig. 5a). By contrast, when we inhibited the lysosomal degradative pathway with leupeptin, an inhibitor of lysosomal enzymes, $P2Y_{13}$-GFP expression was not modified, and the receptor was still poorly detected (Fig. 5a), as in non-treated cells (Fig. 1a). Consistent with these observations, western blot analysis showed that $P2Y_{13}$-GFP was not detected after overexpression in HeLa cells, much like after leupeptin treatment. Conversely, inhibition of proteasome induced a strong expression of $P2Y_{13}$-GFP (Fig. 5b).

Altogether, these data showed that $P2Y_{13}$-R was degraded through the proteasome pathway.

We then investigated the effects of proteasomal inhibition on cell surface expression of $P2Y_{13}$-R in human hepatocytes, using HepG2 cells. When expressed in HepG2

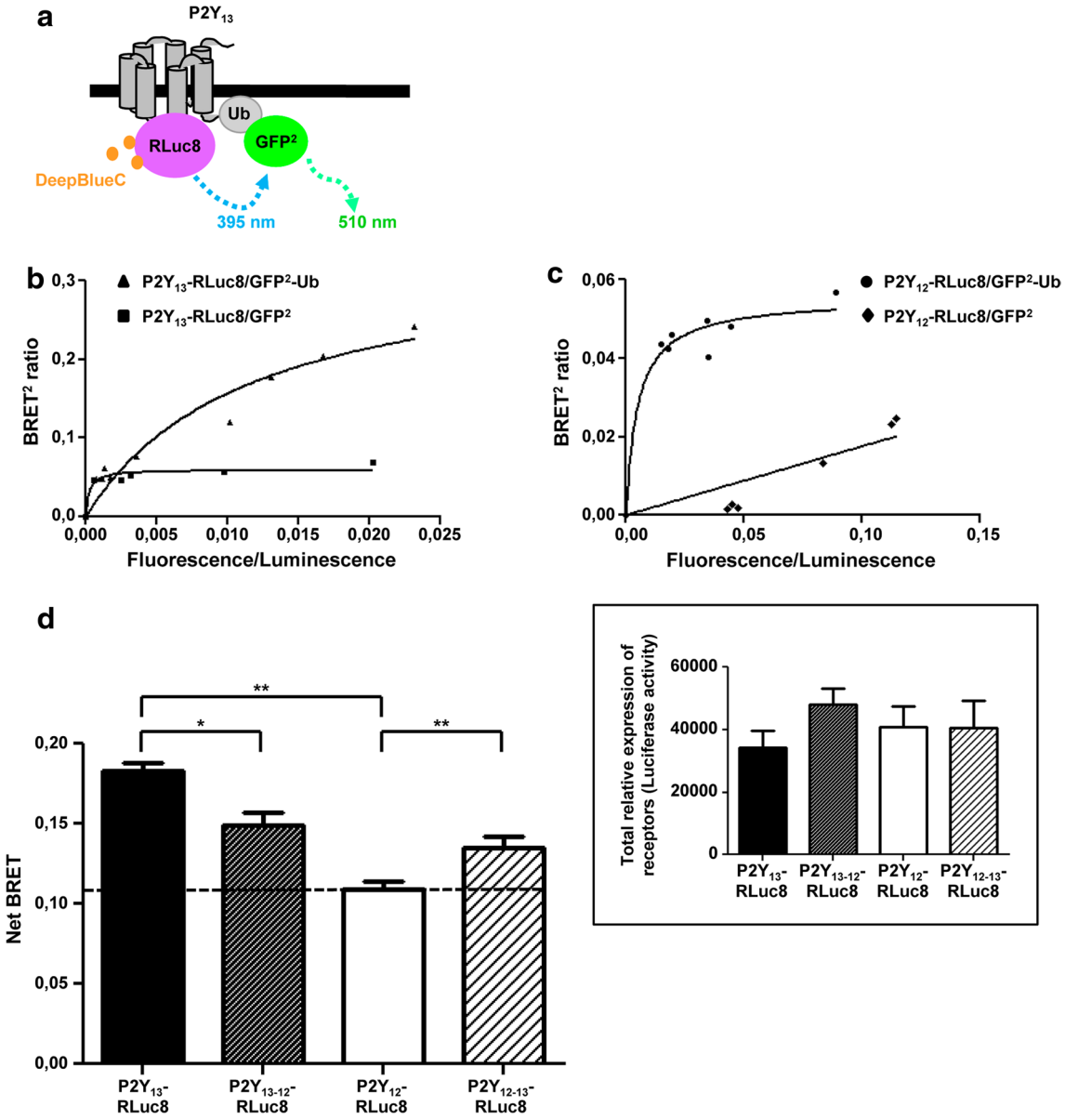

Fig. 3 $P2Y_{13}$ receptor is highly ubiquitinated at steady state. **a** Schematic representation of $BRET^2$ assay between $P2Y_{13}$-RLuc8 and GFP^2-Ub. Upon degradation of its substrate (DeepBlueC coelenterazine), the RLuc8 fused to the C-terminus of the $P2Y_{13}$ receptor emits a blue light with an emission peak at 395 nm. If the $P2Y_{13}$ receptor is ubiquitinated, a nonradiative transfer of energy will occur between RLuc8 and the GFP^2 fused to the N-terminus of ubiquitin, resulting in re-emission of light with an emission peak at 510 nm. HEK293T cells were co-transfected with constant concentrations of $P2Y_{13}$-RLuc8 (**b**) or $P2Y_{13}$-RLuc8 (**c**) DNA constructs and increasing concentrations of plasmids encoding GFP^2-Ub or GFP^2 alone as control. The curves were fitted using a nonlinear regression equation, assuming a single binding site (GraphPad Prism). **d** $BRET^2$ was measured on HEK293T cells co-expressing RLuc8-tagged receptor and GFP^2-Ub. Results are expressed as the mean ± SEM of at least three independent experiments and analyzed by paired *t* test (*$p < 0.05$, **$p < 0.005$). In the *inset*, HEK293T cells were transfected with DNA constructs encoding RLuc8-tagged receptors and luciferase intensity was measured 48 h after transfection. Results are expressed as the mean ± SEM of at least three independent experiments

cells, much like in HeLa cells, $P2Y_{13}$-R was still poorly expressed and mostly detected in the ER as shown by the colocalization with the DsRed2-ER marker (Supplementary Fig S1). In agreement with our results obtained on HeLa cells (Fig. 5a, b), proteasome inhibition with two different specific inhibitors—MG-132 or bortezomib—led to an increase in $P2Y_{13}$-R expression compared to non-treated cells as demonstrated by both fluorescence (Fig. 5c) and western blot (Fig. 5d) experiments. Interestingly, proteasome inhibition induced a striking accumulation of the receptor at the cell surface (Fig. 5c). Expression of $P2Y_{13}$-R at the plasma membrane was further quantified by

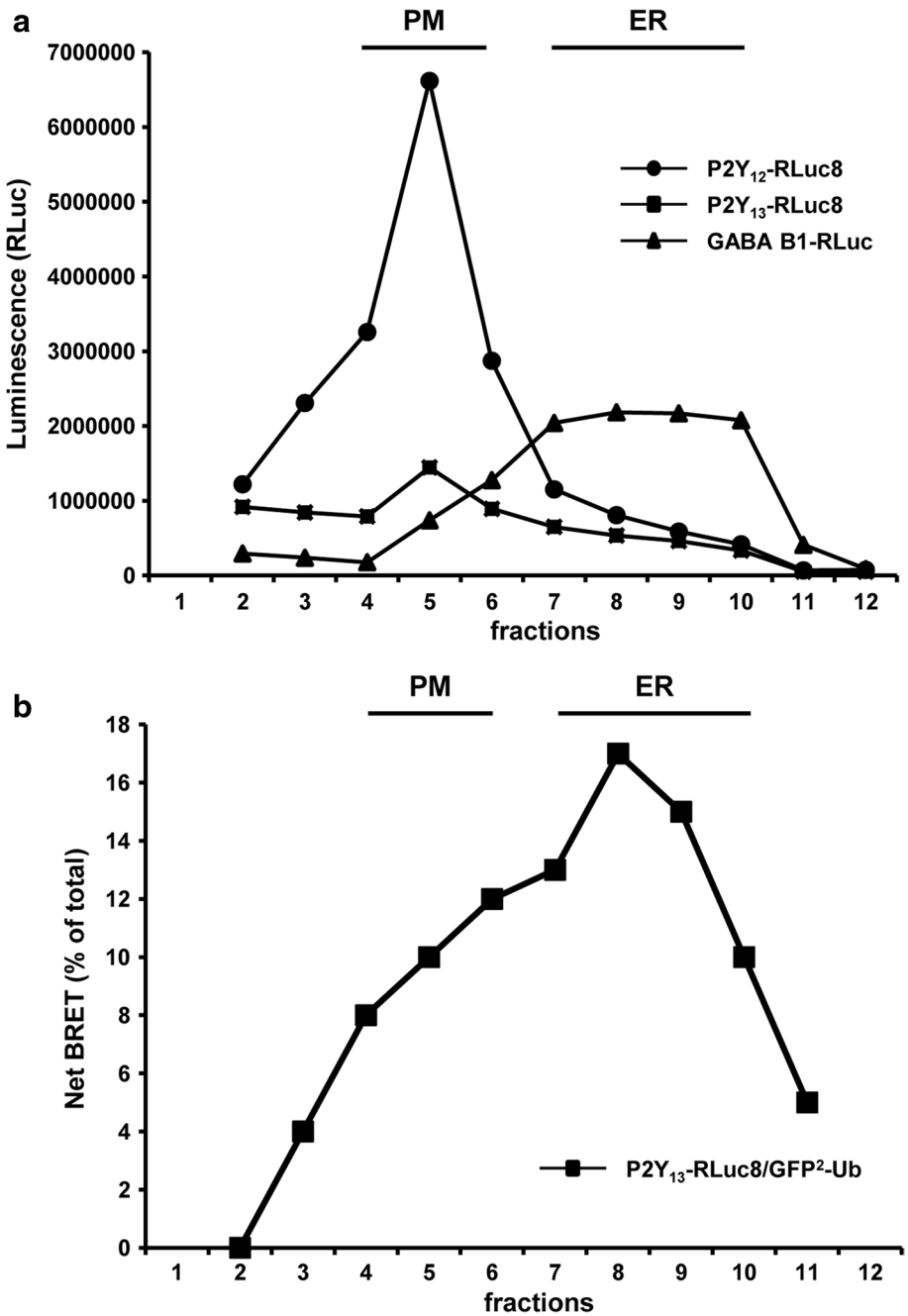

Fig. 4 $P2Y_{13}$ receptor is ubiquitinated in the endoplasmic reticulum HEK293T cells co-expressing RLuc8-tagged receptor and GFP^2-Ub (*filled square*) were lyzed and applied to the top of a discontinuous sucrose gradient. Fractions were collected and subjected to luminescence analysis (**a**) and to BRET measurements (**b**). RLuc8-tagged $P2Y_{12}$ receptor (*filled circle*) and RLuc-fused GABA B1 receptor (*filled triangle*) is used as marker of plasma membrane (*PM*) and endoplasmic reticulum (*ER*), respectively. The subcellular distribution patterns of receptors as well as BRET values are representative of at least three independent experiments

ELISA assay after expression of N-terminally myc-tagged receptor. Both MG-132 and bortezomib treatment induced a significant increase of cell surface expression of $P2Y_{13}$-R (Fig. 5e). Thus, proteasome inhibition on human hepatocytes promotes plasma membrane expression of $P2Y_{13}$-R.

Proteasome inhibition promotes $P2Y_{13}$-mediated hepatic HDL uptake

Since proteasome inhibition induced a strong expression of $P2Y_{13}$-R at the cell surface of hepatocytes (Fig. 5c, e), we first examined HDL uptake in HepG2 cells by using fluorescent HDL_3 after MG-132 treatment. Endocytosis of fluorescent $^{AlexaFluor®568}HDL_3$ particles showed a weak pattern in non-treated hepatocytes. In contrast, when cells were treated with proteasome inhibitor MG-132, the staining was strikingly increased, suggesting that promoting $P2Y_{13}$-R at the cell surface greatly enhanced HDL endocytosis in hepatocytes (Fig. 6a, b).

Therefore, we investigated the hepatic HDL uptake in vivo after bortezomib injection in both wild-type mice and $P2Y_{13}$-R-deficient mice. Hepatic uptake of radiolabeled ^{125}I-HDL_3 in

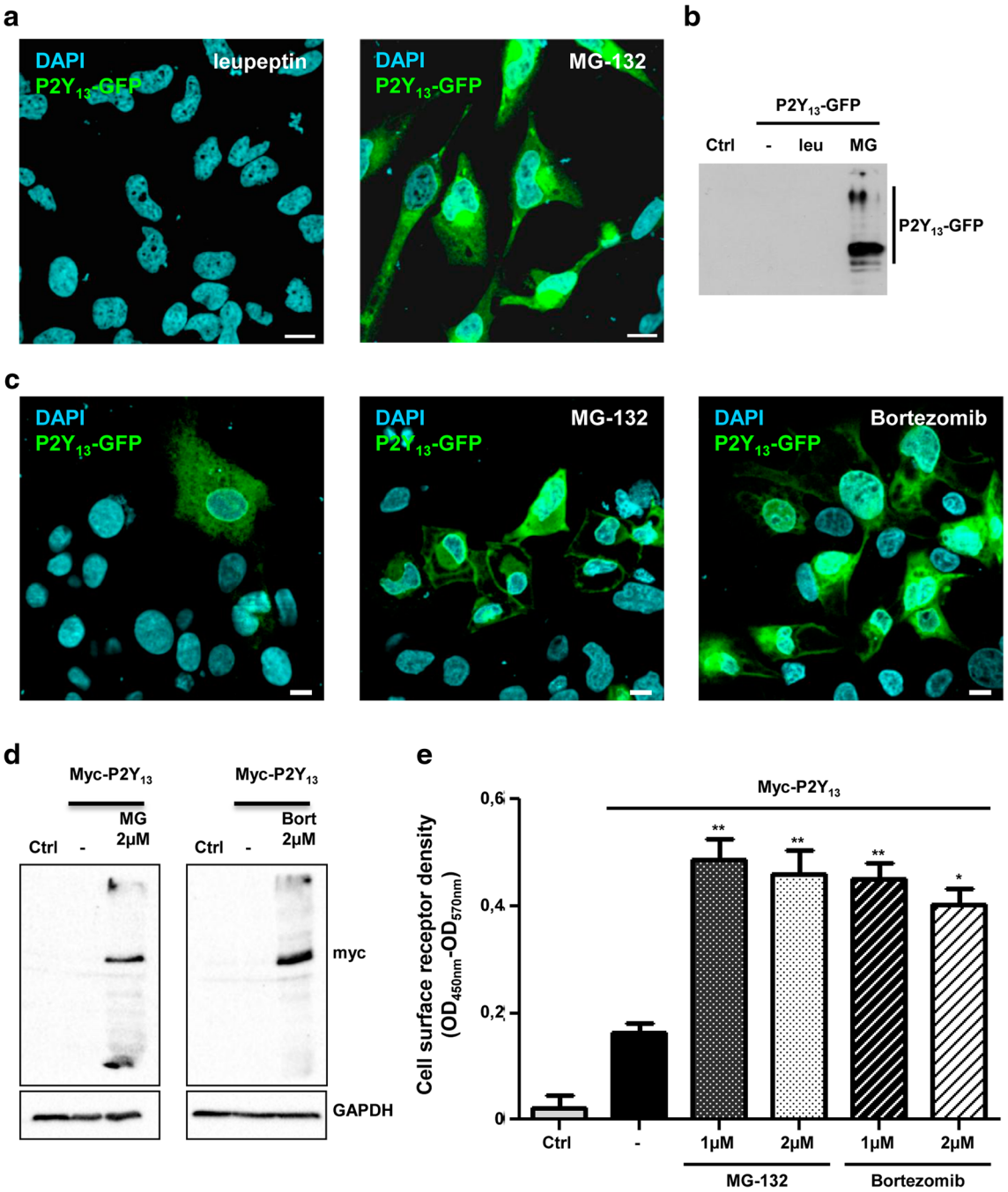

Fig. 5 Proteasome inhibition promotes cell surface expression of $P2Y_{13}$ receptor. **a** HeLa cells expressing $P2Y_{13}$-GFP were treated for 16 h with 250 μg/mL leupeptin or 10 μM MG-132 and then analyzed by fluorescence microscopy. Nuclei were stained with 5 μg/mL DAPI. *Scale bar* 10 μm. **b** HeLa cells expressing $P2Y_{13}$-GFP or not (*Ctrl*) were treated or not (−) for 16 h with 250 μg/mL leupeptin (*leu*) or 10 μM MG-132 (*MG*). Cell lysates were analyzed by SDS gel electrophoresis and western blotting using an anti-GFP antibody. **c** HepG2 cells expressing GFP-tagged $P2Y_{13}$ were treated or not with 2 μM MG-132 or 2 μM bortezomib for 16 h and then analyzed by fluorescence microscopy. Nuclei were stained with 5 μg/mL DAPI. *Scale bar* 10 μm. **d** HepG2 cells expressing N-terminally Myc-tagged $P2Y_{13}$ or not (*Ctrl*) were treated or not (−) with 2 μM MG-132 (*MG*) or 2 μM bortezomib (*Bort*) for 16 h. Cell lysates were then analyzed by SDS gel electrophoresis and western blotting using an anti-myc antibody. GAPDH was used as equal loading marker. (**e**) HepG2 cells expressing or not (Ctrl) N-terminally myc-tagged $P2Y_{13}$ were treated or not (−) with different concentrations of MG-132 or bortezomib for 16 h. Cell surface expression of $P2Y_{13}$ receptor was then analyzed by ELISA using an anti-myc antibody. Results are expressed as the mean ± SEM of at least three independent experiments and analyzed by paired *t* test (*$p < 0.05$, **$p < 0.005$)

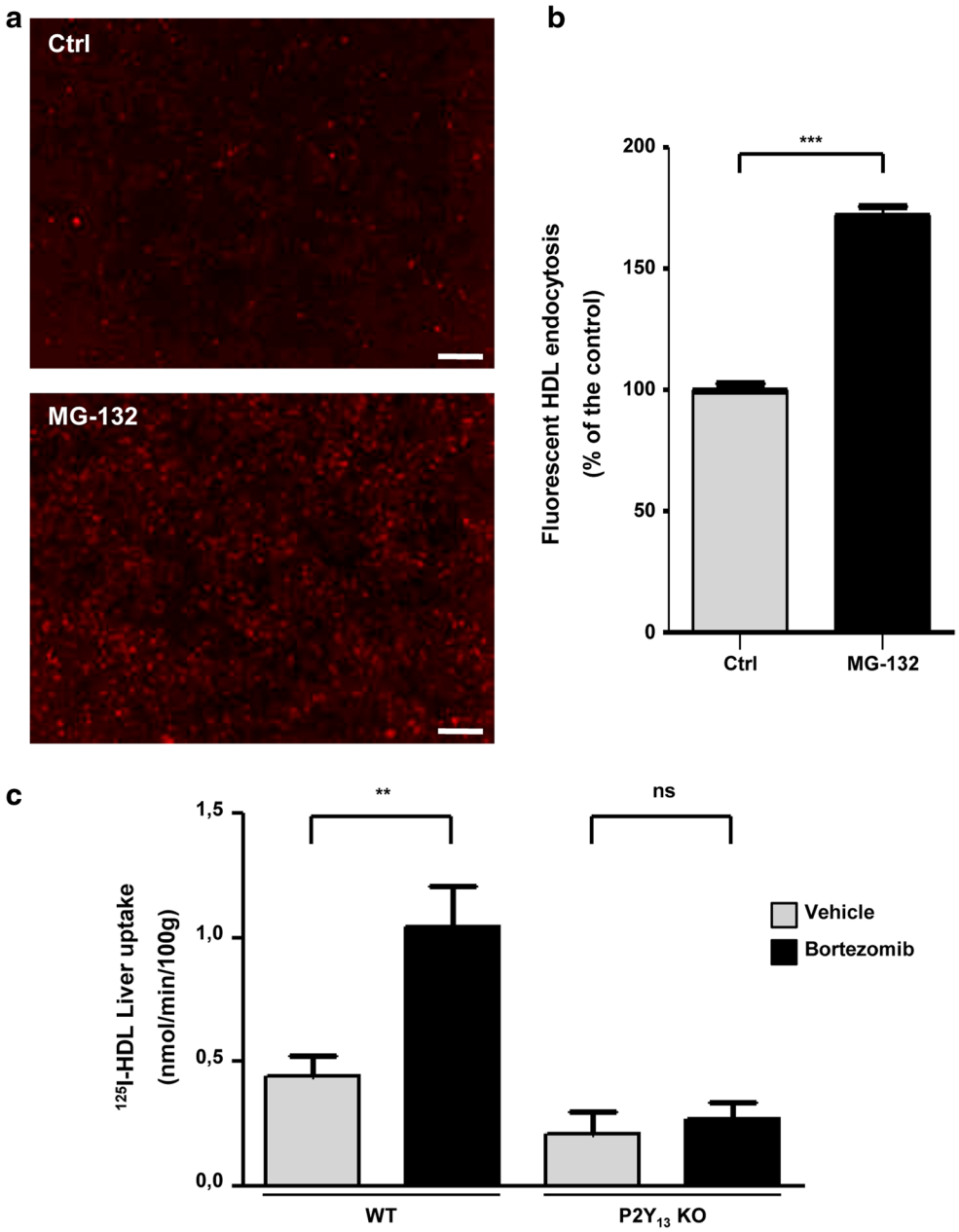

Fig. 6 Proteasome inhibition stimulates $P2Y_{13}$-mediated HDL hepatic uptake. **a** HepG2 cells were treated or not (Ctrl) with 10 μM MG-132 for 16 h, then incubated for 15 min at 37 °C with 100 μg/mL $^{AlexaFluor568®}$-labeled HDL and then analyzed by fluorescence microscopy. *Scale bar* 200 μm. **b** Endocytosis of $^{AlexaFluor568®}$-labeled HDL described in (**a**) was quantified. Results are expressed as the mean ± SEM of at least three independent experiments and analyzed by paired *t* test (***$p < 0{,}001$). **c** Wild-type (*WT*) or $P2Y_{13}$-R knockout mice (*$P2Y_{13}$ KO*) were administered twice at a 5-day interval either 0.5 mg/kg/day bortezomib or the vehicle (saline) by subcutaneous injection. Five days after the second injection, hepatic uptake of radiolabeled ^{125}I-HDL was measured as described in "Materials and methods". Values are expressed as the mean ± SEM. $n = 5$–6 mice at least for each group. Data are analyzed by Mann–Whitney test (**$p < 0{,}005$, *ns* not significant)

wild-type mice was dramatically increased after bortezomib treatment (+233 ± 29 %). Remarkably, proteasome inhibition no longer stimulated HDL uptake in liver from $P2Y_{13}$-R-deficient mice (Fig. 6c), demonstrating that bortezomib-induced hepatic HDL uptake was specifically mediated by $P2Y_{13}$-R.

Altogether, these data suggested that proteasomal inhibition promoted plasma membrane expression of functionally active $P2Y_{13}$-R, and consequently greatly potentiated $P2Y_{13}$-mediated HDL endocytosis by the liver.

Discussion

Regulation of $P2Y_{13}$-R cell surface expression is a key step in modulating hepatic HDL uptake, but the underlying mechanisms remained unknown. In this study, we investigated for the first time the regulation of $P2Y_{13}$-R expression and provided evidence that $P2Y_{13}$-R is tightly regulated by constitutive ubiquitination in the ER, and subsequent proteasome degradation. We also unraveled the role of the C-terminus tail in $P2Y_{13}$-R ubiquitination and plasma membrane expression, since the exchange of the intra-cytoplasmic tail of $P2Y_{13}$-R with the one of $P2Y_{12}$-R led to a concomitant decrease of receptor ubiquitination and an increase of cell surface expression of $P2Y_{13}$-R.

In our previous work, we showed that stimulating $P2Y_{13}$-R activation by using a $P2Y_{13}$-R agonist—namely Cangrelor—stimulated HDL uptake (>34.9 %) [6]. We showed here that proteasome inhibition induced a much more potent up-regulation of HDL endocytosis (>233 %), suggesting that probably, increasing $P2Y_{13}$-R expression at the cell surface—rather than stimulating $P2Y_{13}$-R activation—might be a better way to increase HDL endocytosis. With this in mind, we hypothesized that, in normal conditions, $P2Y_{13}$-R is weakly expressed at the cell surface of hepatocytes, and is responsible for basal hepatic HDL uptake. By contrast, under certain conditions—which are still unknown but which could include fasting or low cholesterol diet—$P2Y_{13}$-R expression might be rapidly and strongly increased at the cell surface to achieve HDL uptake in the liver. Such a tight regulation of $P2Y_{13}$-R expression could be mediated by inhibiting the degradation process through activation/expression of specific deubiquitinating enzymes which would rescue the receptor from proteasome degradation. Alternatively, it is also possible that E3 ubiquitin ligases responsible for receptor ubiquitination were down-regulated. Interestingly, the expression/activation of deubiquitinating enzymes as well as E3 ubiquitin ligases should be fine-tuned, and an increasing number of reports showed that those enzymes could be spatially and temporally regulated during physiological or pathophysiological conditions including embryogenesis or cancer [20, 21].

It is now established that basal ubiquitination and deubiquitination are important for controlling cell surface expression and cellular responsiveness of various GPCR [22]. While ligand-induced ubiquitination usually serves as a sorting signal to target receptor to lysosomal degradation, non-ligand-mediated ubiquitination can relay distinct functions, including regulation of trafficking and receptor density at the cell surface.

Constitutive ubiquitination of GPCR can occur at the plasma membrane to regulate cell surface level of receptors. In *Drosophila*, ubiquitination of the GPCR-related seven transmembrane protein Smo—a signal transducer in Hedgehog signaling—plays a key role in the downregulation of Smo in the absence of the ligand. In the presence of ligand Hedgehog, the deubiquitinating enzyme UBPY/USP8 prevents Smo ubiquitination, thereby promoting Smo accumulation at the cell surface [23, 24]. Similarly, under basal conditions, the chemokine receptor CXCR7 is constitutively ubiquitinated at the cell surface, and activation of CXCR7 by CXCL12 induced a rapid receptor deubiquitination. Importantly, a CXCR7 mutant in which all lysine residues in the C-terminus tail had been replaced by alanines is no longer detected at the cell surface, demonstrating that ubiquitination is a key modification responsible for the correct trafficking of CXCR7 from and to the plasma membrane [25].

However, the ubiquitination status of GPCR can also directly be modulated in the ER, thereby affecting the density of functional receptors at the cell surface and cellular responsiveness. Accordingly, we demonstrated here that the ubiquitination status of $P2Y_{13}$-R in the ER is inversely correlated with cell surface expression. Much like $P2Y_{13}$-R, the adenosine receptor A2A is also subjected to ubiquitination in the ER, promoting subsequent proteasome degradation of functional newly synthesized receptors. Interestingly, the deubiquitinating enzyme USP4 has been shown to deubiquitinate the adenosine receptor A2A during biogenesis, resulting in an increased cell surface expression of functionally active A2A receptor [26]. Hence, proteasome-mediated degradation does not only seem to be restricted to misfolded proteins, and it is tempting to speculate that some properly folded $P2Y_{13}$-R are targeted for proteasome degradation at steady state and released to the cell surface by deubiquitination. Proteasome inhibition might overcome the degradation machinery, leading to the escape of some functional $P2Y_{13}$-R towards the plasma membrane. This would be in agreement with our results showing that proteasomal inhibition drastically potentiated hepatic HDL uptake in wild-type mice but not in $P2Y_{13}$ knock-out mice.

Interestingly, ubiquitin proteasome system has been already described in cholesterol metabolism. Indeed, proteasome inhibition strongly increases protein expression of ATP-binding cassette transporters ABCA1/ABCG1 [27], which both play essential roles in cholesterol efflux from macrophages [28]. Likewise, gp78, another E3 ubiquitin ligase, is involved in the sterol-induced degradation of the enzyme 3-hydroxy-3-methylglutaryl coenzyme A (HMG CoA) reductase in the ER [29, 30]. The HMG CoA reductase catalyzes the rate-limiting reaction of cholesterol synthesis and is inhibited by the statins that are widely used in cholesterol-lowering therapies to reduce the incidence of coronary artery diseases. In this case, gp78-mediated ubiquitination marks the reductase for proteasome degradation when cellular sterol levels rise. Thus,

the ubiquitin–proteasome system seems to regulate central pathways for regulation of cholesterol metabolism and thus might constitute a new attractive target to control dyslipidemia.

In addition, Idol (inductible degrader of the LDL receptor), an E3 ubiquitin ligase, ubiquitinates the precursor of LDL receptor (LDLR), thereby targeting it for degradation. Consequently, Idol knockdown in hepatocytes increases LDLR protein levels and promotes LDL uptake [31]. Hence, given the importance of both HDL- and LDL-cholesterol metabolism in cardiovascular disease risk, a better understanding of those ubiquitin-regulated pathways could lead to new therapeutic opportunities.

In addition to ubiquitination, many additional/complementary mechanisms could limit surface expression of $P2Y_{13}$-R as already described for many other GPCR. In particular, some receptors might necessitate the specialized assistance of general or specific chaperone/escort proteins in the ER to fold properly and exit from the ER to navigate towards the Golgi [32]. Glycosylation may also represent an absolute requirement for the cell surface expression of some GPCR. Thus, mutations in the glycosylation sites of AT1a angiotensin II receptor resulted in the retention of mutated receptors in the ER [33]. Finally, homo- or heterodimerization has now been well described to participate to the proper export of some GPCR to the plasma membrane and might represent a prerequisite to pass quality-control checkpoints along the biosynthetic pathway. Interestingly, olfactory receptors, which are notoriously difficult to express on their own, reached the plasma membrane upon heterodimerization with the β2-adrenoceptor [34].

We previously studied pharmacological activation of the $P2Y_{13}$-R by its partial agonist, the Cangrelor. Of note, we demonstrated that Cangrelor administration in mice could promote hepatic HDL endocytosis and biliary lipid excretion and might thus represent a new therapeutic approach to improve hepatobiliary RCT [6, 8]. However, the lack of oral bioavailability of Cangrelor and its very short half-life, as well as its antagonistic action on $P2Y_{12}$-R, preclude its clinical use. It will therefore be a tremendous challenge to develop an uncharged agonist of $P2Y_{13}$-R suitable for oral administration. An alternative and attractive way to stimulate $P2Y_{13}$-R pathway for HDL endocytosis would be to increase the expression of functional $P2Y_{13}$-R by selectively targeting the ubiquitin–proteasome system that recognizes the receptor as a substrate and thus rescuing $P2Y_{13}$-R from its proteasome degradation. In this context, identification of E3 ligase or deubiquitinating enzymes specific for the regulation of $P2Y_{13}$-R ubiquitination in the ER might provide the basis for a novel therapeutic strategy to enhance hepatobiliary RCT and ultimately prevent or treat atherosclerosis.

Acknowledgments We thank Nabila Mansouri for technical assistance. We also thank Sophie Allart and Astrid Canivet for technical assistance at the cellular imaging facility (INSERM UMR 1043, Toulouse), the technical service of the animal facility (Genotoul Anexplo Platform) and the DNA sequencing platform (Plateau de génomique GeT-Purpan de la plateforme Génome et Transcriptome de la génopole de Toulouse). This study was supported by the INSERM Avenir Grant, the National Research Agency (ANR Emergence and GENO #102 01) and the Midi-Pyrénées Region. Véronique Pons was supported by the Fondation pour La Recherche Médicale (FRM) and INSERM.

Conflict of interest None.

References

1. Yvan-Charvet L, Matsuura F, Wang N et al (2007) Inhibition of cholesteryl ester transfer protein by torcetrapib modestly increases macrophage cholesterol efflux to HDL. Arterioscler Thromb Vasc Biol 27:1132–1138
2. Acton S, Rigotti A, Landschulz KT et al (1996) Identification of scavenger receptor SR-BI as a high density lipoprotein receptor. Science 271:518–520
3. Martinez LO, Jacquet S, Esteve J et al (2003) Ectopic b -chain of ATP synthase is an apolipoprotein A-I receptor in hepatic HDL endocytosis. Nature 421:75–79
4. Jacquet S, Malaval C, Martinez LO et al (2005) The nucleotide receptor P2Y13 is a key regulator of hepatic high-density lipoprotein (HDL) endocytosis. Cell Mol Life Sci 62:2508–2515
5. Malaval C, Laffargue M, Barbaras R et al (2009) RhoA/ROCK I signalling downstream of the P2Y13 ADP-receptor controls HDL endocytosis in human hepatocytes. Cell Signal 21:120–127
6. Fabre AC, Malaval C, Ben Addi A, et al. (2010) P2Y13 receptor is critical for reverse cholesterol transport. Hepatology 52: 1477–83
7. Blom D, Yamin T-T, Champy M-F et al (2010) Altered lipoprotein metabolism in P2Y(13) knockout mice. Biochim Biophys Acta 1801:1349–1360
8. Serhan N, Cabou C, Verdier C et al (2013) Chronic pharmacological activation of P2Y13 receptor in mice decreases HDL-cholesterol level by increasing hepatic HDL uptake and bile acid secretion. Biochim Biophys Acta 1831:719–725
9. Communi D, Gonzalez NS, Detheux M et al (2001) Identification of a novel human ADP receptor coupled to G(i). J Biol Chem 276:41479–41485
10. Yano S, Tsukimoto M, Harada H, Kojima S (2012) Involvement of P2Y13 receptor in suppression of neuronal differentiation. Neurosci Lett 518:5–9
11. Amisten S, Meidute-Abaraviciene S, Tan C et al (2010) ADP mediates inhibition of insulin secretion by activation of P2Y13 receptors in mice. Diabetologia 53:1927–1934
12. Gao Z-G, Ding Y, Jacobson K (2010) P2Y(13) receptor is responsible for ADP-mediated degranulation in RBL-2H3 rat mast cells. Pharmacol Res 62:500–505
13. Wang L, Olivecrona G, Götberg M et al (2005) ADP acting on P2Y13 receptors is a negative feedback pathway for ATP release from human red blood cells. Circ Res 96:189–196
14. Wang N, Robaye B, Agrawal A (2012) Reduced bone turnover in mice lacking the P2Y13 receptor of ADP. Mol Endocrinol 26:142–152
15. Terrillon S, Durroux T, Mouillac B, et al. (2003) Oxytocin and vasopressin V1a and V2 receptors form constitutive homo- and heterodimers during biosynthesis. Mol Endocrinold) 17: 677–91

16. Vembar S, Brodsky J (2008) One step at a time: endoplasmic reticulum-associated degradation. Nat Rev Mol Cell Biol 9:944–957
17. Perroy J, Pontier S, Charest PG et al (2004) Real-time monitoring of ubiquitination in living cells by BRET. Nat Methods 1:203–208
18. Mercier J-F, Salahpour A, Angers S et al (2002) Quantitative assessment of beta 1- and beta 2-adrenergic receptor homo- and heterodimerization by bioluminescence resonance energy transfer. J Biol Chem 277:44925–44931
19. Margeta-mitrovic M, Jan YN, Jan LY, Francisco S (2000) GABA B receptor heterodimerization. Neuron 27:97–106
20. Seliger B, Fedorushchenko A, Brenner W et al (2007) Ubiquitin COOH-terminal hydrolase 1: a biomarker of renal cell carcinoma associated with enhanced tumor cell proliferation and migration. Clin Cancer Res 13:27–37
21. Li D, Zhang J, Huang W et al (2013) Up-regulation of Smurf1 after spinal cord injury in adult rats. J Mol Histol 44:381–390
22. Dores MR, Trejo J (2012) Ubiquitination of G protein-coupled receptors: functional implications and drug discovery. Mol Pharmacol 82:563–570
23. Xia R, Jia H, Fan J et al (2012) USP8 promotes smoothened signaling by preventing its ubiquitination and changing its subcellular localization. PLoS Biol 10:e1001238
24. Li S, Chen Y, Shi Q et al (2012) Hedgehog-regulated ubiquitination controls smoothened trafficking and cell surface expression in Drosophila. PLoS Biol 10:e1001239
25. Canals M, Scholten DJ, De Munnik S et al (2012) Ubiquitination of CXCR7 controls receptor trafficking. PLoS ONE 7:e34192
26. Milojevic T, Reiterer V, Stefan E et al (2006) The ubiquitin-specific protease Usp4 regulates the cell surface level of the A 2a receptor. Mol Pharmacol 69:1083–1094
27. Ogura M, Ayaori M, Terao Y et al (2011) Proteasomal inhibition promotes ATP-binding cassette transporter A1 (ABCA1) and ABCG1 expression and cholesterol efflux from macrophages in vitro and in vivo. Arterioscler Thromb Vasc Biol 31:1980–1987
28. Cavelier C, Lorenzi I, Rohrer L, Von Eckardstein A (2006) Lipid efflux by the ATP-binding cassette transporters ABCA1 and ABCG1. Biochim Biophys Acta 1761:655–666
29. Song B-L, Sever N, DeBose-Boyd R (2005) Gp78, a membrane-anchored ubiquitin ligase, associates with Insig-1 and couples sterol-regulated ubiquitination to degradation of HMG CoA reductase. Mol Cell 19:829–840
30. Jo Y, Lee PCW, Sguigna PV, DeBose-Boyd R (2011) Sterol-induced degradation of HMG CoA reductase depends on interplay of two INSIGs and two ubiquitin ligases, gp78 and Trc8. Proc Natl Acad Sci USA 108:20503–20508
31. Zelcer N, Hong C, Boyadjian R, Tontonoz P (2009) LXR regulates cholesterol uptake through Idol-dependent ubiquitination of the LDL receptor. Science 325:100–104
32. Achour L, Labbé-Jullié C, Scott MGH, Marullo S (2008) An escort for GPCRs: implications for regulation of receptor density at the cell surface. Trends Pharmacol Sci 29:528–535
33. Deslauriers B, Ponce C, Lombard C et al (1999) N-glycosylation requirements for AT1a angiotensin II receptor delivery to the plasma membrane. Biochem J 339:397–405
34. Hague C, Uberti M, Chen Z et al (2004) Olfactory receptor surface expression is driven by association with the beta2-adrenergic receptor. Proc Natl Acad Sci USA 101:13672–13676